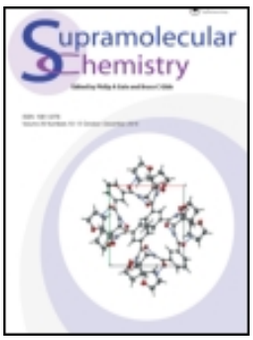

Supramolecular Chemistry

ISSN: 1061-0278 (Print) 1029-0478 (Online) Journal homepage: http://www.tandfonline.com/loi/gsch20

Molecular recognition of amphiphilic p-sulfonatocalix[4]arene with organic ammoniums

Xin-Yue Hu, Shu Peng, Dong-Sheng Guo, Fei Ding & Yu Liu

To cite this article: Xin-Yue Hu, Shu Peng, Dong-Sheng Guo, Fei Ding & Yu Liu (2015) Molecular recognition of amphiphilic p-sulfonatocalix[4]arene with organic ammoniums, Supramolecular Chemistry, 27:5-6, 336-345, DOI: 10.1080/10610278.2014.967242

To link to this article: http://dx.doi.org/10.1080/10610278.2014.967242

Supramolecular Chemistry, 2015
Vol. 27, Nos. 5–6, 336–345, http://dx.doi.org/10.1080/10610278.2014.967242

Molecular recognition of amphiphilic *p*-sulfonatocalix[4]arene with organic ammoniums

Xin-Yue Hu, Shu Peng, Dong-Sheng Guo, Fei Ding and Yu Liu*

State Key Laboratory of Elemento-Organic Chemistry, Department of Chemistry, Nankai University, Collaborative Innovation Center of Chemical Science and Engineering (Tianjin), Tianjin 300071, P.R. China

(*Received 16 June 2014; accepted 16 September 2014*)

The binding abilities and thermodynamic origin for the intermolecular complexation of two water-soluble calixarenes, *p*-sulfonatocalix[4]arene (SC4A) and 5,11,17,23-tetrasulfonato-25,26,27,28-tetrakis(*n*-butyl)-calix[4]arene (SC4A-Bu), with six organic cations: 1,4-diazabicyclo[2,2,2]octane (G1), 3,5,6,8,-tetrahydropyrazino[1,2,3,4-Imn][1,10]phenanthroline (G2), diquat (G3), paraquat (G4), 1-methylpyridin-1-ium (G5) and 1,3-dimethylimidazolium (G6), have been determined by means of isothermal titration calorimetry in aqueous solutions at pH 7.0, 298.15 K, and their binding modes have been investigated by NMR spectroscopy. The obtained results indicate that the binding modes of SC4A-Bu and SC4A change a little but their binding affinities show great difference, resulting from the distinguishable binding thermodynamics. The binding selectivity of G1 is up to 688 times for the SC4A/SC4A-Bu hosts, and SC4A-Bu prefers to include planer molecules of large π system with low electron density. The aggregation behaviours of SC4A-Bu before and after complexation with G3 were then investigated, showing that G3 is able to induce the aggregation of SC4A-Bu.

Keywords: calixarene; recognition; thermodynamics; amphiphile; ammonium

Introduction

p-Sulfonatocalix[*n*]arenes (SC*n*As) are a prominent family of water-soluble calixarene derivatives, which were first reported by Shinkai et al. (*1*). Up to now, SC*n*As have gained more and more attention in supramolecular chemistry and other disciplines for exactly 30 years, benefiting from their advantageous features (*2*). First, they are easy to be prepared as sulfonation could directly happen on the upper rim of calixarene with satisfied yields. Second, they have high water solubility, and the driving forces for guest inclusion in the cavity, such as hydrophobic and π-stacking interactions, are more effective in aqueous media than in organic media. Third, the upper-rim sulfonate groups provide synergistical anchoring points besides the intrinsic π-electron-rich cavities, which enable SC*n*As to display especially strong binding ability and high molecular selectivity towards a variety of organic ions (*3–6*). Finally, SC*n*As are biocompatible (*7–10*). These advantages bring SC*n*As about diverse applications in molecular recognition/sensing (*11*, *12*), crystal engineering (*13*, *14*), catalysis (*15*), supra-amphiphiles (*16*), enzyme-mimics/enzyme-assays (*17–21*) and medicinal chemistry (*22*, *23*).

Grafting hydrophobic alkyl chains at the lower rim generates SC*n*As derivatives with amphiphilic properties. Calixarene amphiphiles consist of multiple lipophilic groups at one rim and multiple hydrophilic groups at the other rim, which are covalently linked by methylene bridges, representing a type of preorganised cyclic oligomer of amphiphiles (*24*, *25*). From the viewpoint of structural features, they incorporate both gemini-type and bola-type amphiphiles into a single molecule (*26*). As a result, calixarene amphiphiles exhibit some special assembling properties that cannot be easily obtained by other traditional amphiphiles (*27*), including low critical aggregation concentration (CAC) (*28*), high stability (*29*) and slow exchange kinetics (*30*).

One more significant characteristic of calixarene amphiphiles should be concerned is the cavity binding property, which can be described as 'surfactants with a host–guest recognition site'. Calixarene amphiphiles form assemblies with special binding sites (calixarene cavity) on their outer-layer surface, which could be further non-covalently coronated and hierarchically assembled (*26*, *31*). We have reported a amphiphilic co-assembly between *p*-sulfonatocalix[4]arene tetraheptyl ether and chlorpromazine. Due to the host–guest recognition site on the outer-layer surface, a targeting agent – trimethylated chitosan – could be further anchored on the constructed nanoparticle for targeted delivery (*26*). Meanwhile, inclusion of guests may affect the assembling behaviour of calixarene amphiphiles (*32*, *33*), like the calixarene-induced aggregation cases that complexation with SC*n*As promotes the aggregation of aromatic or amphiphilic guest molecules (*34–40*). It is reasonably acceptable that the size/shape and hydrophilicity of the polar headgroups, as well as the

*Corresponding author. Email: yuliu@nankai.edu.cn

electrostatic repulsion between the headgroups, were adjusted by guest binding into cavity. However, previous works have paid much attention to the advantages of facile modification and preorganised macrocyclic scaffold of calixarenes on building novel artificial amphiphiles (*41–44*), while the cavity effect has almost been ignored.

Before guest-regulated amphiphilic aggregation studies, it is crucial to first investigate the inclusion properties of amphiphilic calixarenes to help us understand how and to what extent the complexation of guest into cavity affect the aggregation behaviour of amphiphilic calixarenes. In this study, we investigated the inclusion behaviour of *p*-sulfonatocalix[4]arene tetrabutyl ether (SC4A-Bu) with six model guests (G1–G6) by means of NMR spectroscopy and isothermal titration calorimetry (ITC), which was comparatively discussed with the *p*-sulfonatocalix[4]arene (SC4A) results from the viewpoints of binding geometry, affinity and thermodynamic origin (Scheme 1). Although molecular recognition of lower-rim modified SC*n*As has been pursued before by our group and others (*45–49*), the present work is novel and valuable in view of amphiphilic assembly adjusted by guest complexation. Furthermore, based on these recognition results, amphiphilic aggregations of SC4A-Bu in the absence and presence of G3 were evaluated.

Results and discussion

Binding structures by NMR spectroscopy

NMR spectroscopy has been widely used to determine the structures of calixarene complexes by analysing complexation-induced shifts. The protons of encapsulated guests shift upfield ($\Delta\delta = \delta_{complex} - \delta_{free} < 0$) owing to the ring current effect of the aromatic nuclei of Sc*n*As (*50*). So in order to get information about the possible complex structures of SC4A-Bu with six guests, ^{1}H NMR spectra of G1–G6 in the absence and presence of SC4A-Bu were measured at pD 7.0. The ^{1}H NMR spectra of the G3–G6 guests with SC4A at the same condition were recorded in our previous work (*5*, *51*).

In the ^{1}H NMR spectra, the proton signal of methylene bridge in SC4A presents a sharp mono-peak, indicating the flexible cone conformation in which the aromatic rings flipped rapidly on the NMR time scale (*4*). Upon complexation with guests, the proton signal becomes obtuse (*5*, *51*), which provides the evidence for the complexation-induced conformational rigidification of SC4A. The protons of methylene bridge in SC4A-Bu present two groups of peaks assigned to the axial and equatorial protons, respectively (*6*), because the lower-rim modification leads to the rigidified pinch-cone conformation adopted by SC4A-Bu. There is no conspicuous difference of proton signals when it complexed with guest molecules, which proves that the rigidified SC4A-Bu did not afford the structural compensation to capture guests as flexible as SC4A (*6*). Meanwhile, according to our previous research (*6*), SC4A-Bu assumes a pinched-cone conformation of C_{2v} symmetry in the solid state, having distances between the two pairs of sulfonate groups (S···S) of 5.15 and 12.95 Å, in contrast to the reported C_{4v}-symmetrical cone conformation of SC4A with equal S···S distances of about 10 Å, which means that SC4A-Bu and SC4A would show different binding geometries towards different guests.

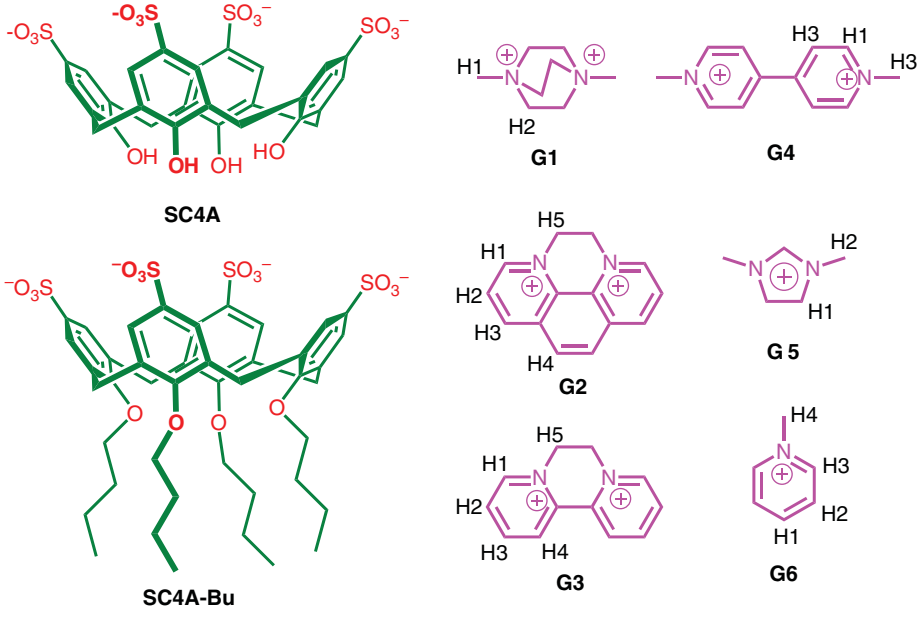

Scheme 1. (Colour online) Structures of the employed SC4A and SC4A-Bu hosts and G1–G6 guests.

Table 1. Chemical shift changes ($\Delta\delta$, ppm) of G1 − G6 in the presence of SC4A-Bu or SC4A.[a]

	G1	G2	G3	G4	G5	G6
SC4A[b]	H1 −1.99	H1 −0.91	H1 −1.03	H1 −1.21	H1 −1.10	H1 −3.25
	H2 − 0.98	H2 −1.52	H2 −1.64	H2 −0.62	H2 −3.02	H2 −2.53
		H3 −1.61	H3 −1.52	H3 −1.52		H3 −1.65
		H4 −1.05	H4 −0.99			H4 −0.75
		H5 −0.15	H5 −0.36			
SC4A-Bu	H1 − 1.34	H1 −1.40	H1 −0.95	H1 −1.21	H1 −0.65	H1 −1.375
	H2 − 0.32	H2 −2.01	H2 −2.41	H2 −0.25	H2 −2.11	H2 −1.511
		H3 −1.59	H3 −2.65	H3 − 1.33		H3 −0.973
		H4 −0.83	H4 −1.04			H4 −0.397
		H5 −0.35	H5 − 0.35			

[a] $\Delta\delta = \delta$ (presence of 1 equiv. host) $- \delta$ (free guest). Negative values indicate upfield shift.
[b] The $\Delta\delta$ values of SC4A with G3–G6 are from our previous work, Ref. (*5*).

The complexation-induced chemical shifts of G1–G6 were listed in Table 1. For G1, the $\Delta\delta$ values are in the same order of H1 > H2 upon addition of SC4A and SC4A-Bu (Figure 1). According to the ^{1}H NMR data, two possible binding manners could be assumed: G1 was immersed into the calixarene cavity with a vertical or horizontal manner. Therefore, 2D NMR spectra were taken to give more information about the binding geometry. Rotating frame overhauser effect Spectroscopy (ROESY) cross-peaks are indicative of specific proximity relationships between host and guest protons (generally 4 Å or less) (*4*). As can be seen from Figure 2(a), the ROESY spectrum of the SC4A-Bu + G1 complex exhibits clear cross-peaks between G1 protons and aromatic protons (Ar—H) of SC4A-Bu, and the cross-peak of H2 and Ar—H is weaker than that of H1, which means that H1 is more adjacent to Ar—H than H2. The vertical manner was reasonably eliminated, in which H1 should be more away from Ar—H than H2. The horizontal manner of complexation of calixarenes with G1 is illustrated in Figure 3. Important to note, SC4A-Bu leads to smaller $\Delta\delta$ values of G1 than SC4A. It may be involved in three probable reasons. First, there are still some free G1 molecules that were not captured by SC4A-Bu; second, SC4A-Bu affords a weaker ring current effect when binding guests; third, the inclusion depth of SC4A-Bu with G1 is shallower than that of SC4A. The first reason could be eliminated by the following complexation stability constants (K_S, Table 2) that all G1 molecules should be

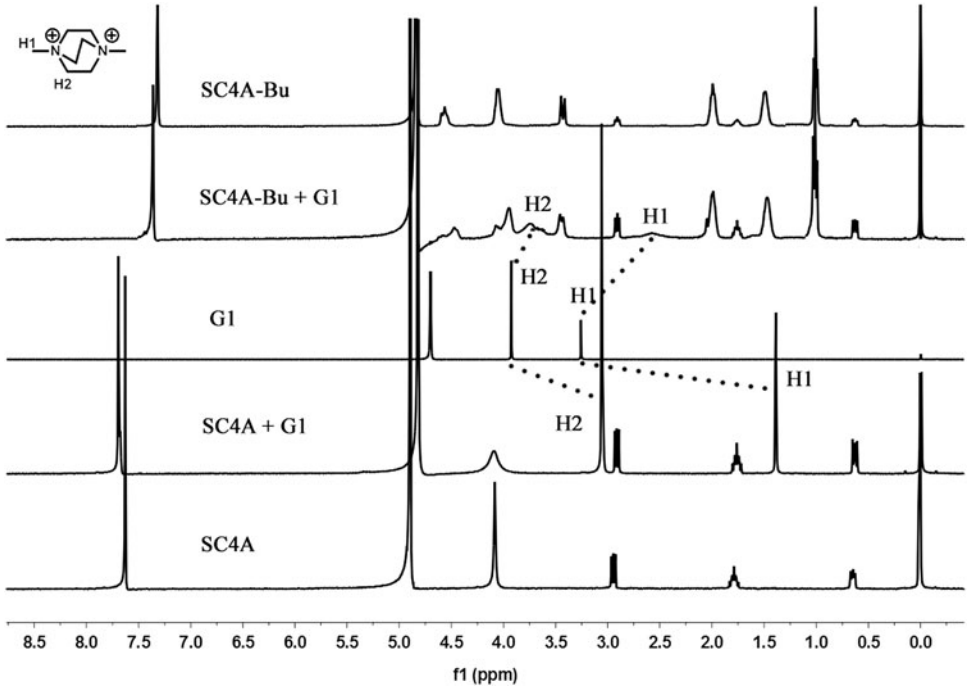

Figure 1. The ^{1}H NMR spectra (400 MHz, D_2O, 25°C) of G1 (2.0 mM) in the absence and presence of 1 equiv. SC4A or SC4A-Bu at pD 7.0. '◆' represents DSS signals.

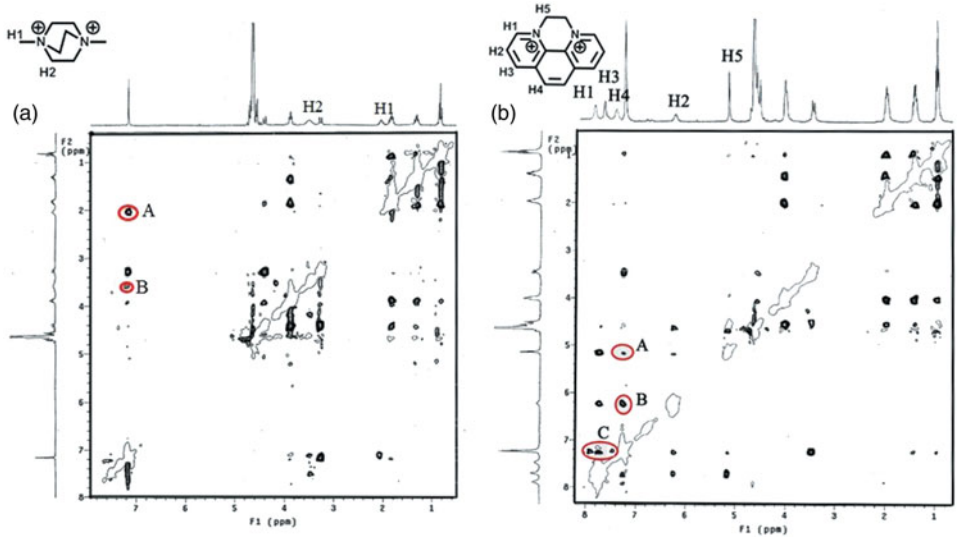

Figure 2. (Colour online) The 2D ROESY spectra of SC4A-Bu + G1 (a) and SC4A-Bu + G2 (b) with a mixing time of 250 ms. The concentrations of host and guest are at 2.0 mM.

bonded to SC4A-Bu under the NMR condition. Moreover, the complexation of SC4A-Bu induces larger $\Delta\delta$ values for G3 than SC4A, and therefore the second reason is not the rational explanation. For the third reason, it was further validated by the following ITC measurements.

The $\Delta\delta$ values of G2 are in the order of H3 $\approx$ H2 $>$ H1 $\approx$ H4 $>$ H5 in the presence of SC4A, while in the order of H2 $>$ H3 $>$ H1 $>$ H4 $>$ H5 in the presence of SC4A-Bu. The results indicate that G2 was immersed into the cavities of SC4A in an acclivitous orientation with the aromatic moiety included first. When complexed with SC4A-Bu, the order of $\Delta\delta$ values did not change so much, but H2 shows a larger $\Delta\delta$ value than H3, and H1 show a larger shift value than H4, which means H2 (H1) immersed deeper than H3 (H4) when complexed with SC4A-Bu. The similar results were also obtained by the ROESY experiment. According to the ROESY spectrum (Figure 2(b)), all protons show obvious cross-peaks with Ar—H of SC4A-Bu, while H4 and H5 show a weaker cross-peak than H1, H2 and H3, which indicate H1, H2

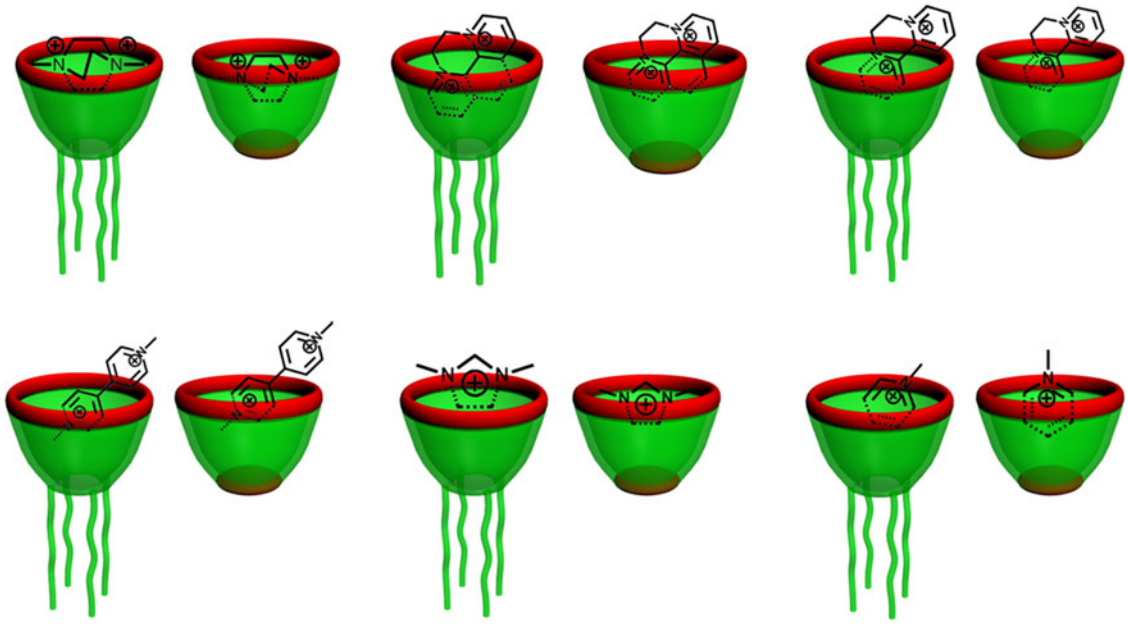

Figure 3. Schematic illustration of the deduced binding manners of SC4A-Bu or SC4A with guests G1–G6 according to NMR spectra, which represents an average of a dynamic ensemble.

Table 2. Complex stability constants (KS), enthalpy (ΔH°) and entropy ($T\Delta S^\circ$) changes for the 1:1 complexation[a] of SC4A and SC4A-Bu with G1 − G6 at 298.15 K, pH 7.0.

Entry	Host	Guest	ΔH° (kJ mol^{-1})	$T\Delta S^\circ$ (kJ mol^{-1})	K_S (M^{-1})
1	SC4A-Bu	G1	−4.9 ± 0.1	19.8 ± 0.1	(2.2 ± 0.1) × 10^4
2		G2	−35.4 ± 0.2	9.1 ± 0.1	(7.0 ± 0.1) × 10^7
3		G3	−35.3 ± 0.2	9.9 ± 0.2	(2.5 ± 0.1) × 10^7
4		G4	−29.9 ± 0.2	4.4 ± 0.2	(1.0 ± 0.2) × 10^6
5		G5	−42.2 ± 0.1	−17.3 ± 0.2	(2.3 ± 0.1) × 10^4
6		G6	−31.8 ± 0.1	−3.5 ± 0.1	(9.1 ± 0.1) × 10^4
7	SC4A	G1	−22.9 ± 0.1	18.0 ± 0.1	(1.5 ± 0.1) × 10^7
8		G2	−37.6 ± 0.1	−2.6 ± 0.1	(1.9 ± 0.1) × 10^7
9		G3	−29.4 ± 0.1	13.9 ± 0.1	(4.3 ± 0.1) × 10^7
10		G4[b]	−27.2	6.8	9.3 × 10^5
11		G5[b]	−28.0	3.2	2.9 × 10^5
12		G6[b]	−31.2	1.9	6.4 × 10^5

[a] All ITC titrations revealed a 1:1 binding stoichiometry from the curve fitting.
[b] Data from Ref. (*5*).

and H3 are closer to the Ar—H than H4 and H5. These results suggest that G2 also immersed into the cavities of SC4A-Bu in an acclivitous orientation, but may be a little more vertical compared with SC4A.

The $\Delta\delta$ values of G3, G4 and G5 were almost in the same order when included by either SC4A or SC4A-Bu, H3 ≈ H2 > H4 ≈ H1 > H5 for G3, H3 > H1 > H2 for G4 and H2 > H1 for G5. It is reasonable to think that the binding geometries are similar when G3–G5 are binding with these two hosts. The deduced binding manners are shown in Figure 3. The $\Delta\delta$ values of G6 are in the order of H1 > H2 > H3 > H4 in the presence of SC4A, while in the order of H2 > H1 > H3 > H4 in the presence of SC4A-Bu. The sequence between H1 and H2 is overturned. In our previous work (*5*), we inferred that the aromatic portion of G6 was vertically immersed into the cavity of SC4A with the positively charged N—CH_3 located at the upper rim composed of sulfonate groups. In the present SC4A-Bu case, a binding geometry of acclivitous orientation was preferred, as shown in Figure 3. It is reasonably acceptable that the pinched-cone SC4A-Bu could accommodate aromatic planer guests in more horizontal orientation than the cone SC4A. It is also notable that SC4A-Bu leads to obviously smaller $\Delta\delta$ values of G6 than SC4A. Resembling the G1 case, the inclusion of SC4A-Bu with G6 is shallower than that of SC4A. Comparing with the binding manner of SC4A with G6, SC4A-Bu adopts a more horizontal and shallower manner.

Binding ability and thermodynamics

To determine quantitatively the inclusion complexation behaviours of SC4A and SC4A-Bu with G1–G6, ITC experiments were performed in neutral aqueous solution. ITC is a powerful tool to determine the host–guest complex interactions, because it not only gives the complex stability constants (K_S) but also yields their thermodynamic parameters (enthalpy and entropy changes ΔH°, ΔS°). The data obtained were listed in Table 2. All the microcalorimetric experiments showed typical titration curves of 1:1 complex formation. The stoichiometric ratios (N values) that we observed from curve-fitting results of the binding isotherm fell within the range of 0.90–1.10:1, which indicates that the host–guest complexes had a 1:1 stoichiometry. The titration data could be fitted well by computer simulation using the 'one set of binding sites' model and repeated as 1:1 complex formation, such that higher-order complexes did not need to be considered. It is reported that free SC4A-Bu shows a CAC of 3.18 mM (*28*). So in order to prevent the aggregation of SC4A-Bu during the ITC experiments, the concentration of SC4A-Bu was fixed at 0.1 mM, which is not only far from the free CAC value but also below the aftermentioned CAC value upon complexation with guests.

As can be seen from Table 2, the most intriguing phenomenon is the binding selectivity for G1 between SC4A and SC4A-Bu. SC4A presents a much stronger binding affinity than SC4A-Bu with a host selectivity of 688 times, reflecting from the dominant enthalpy term ($\Delta\Delta H^\circ_{\text{SC4A-Bu–SC4A}} = 17.9$ kJ mol^{-1}). As demonstrated in the NMR section, SC4A-Bu assumes the rigidified pinched-cone conformation, which is unsuitable to accommodate spherical molecules like G1. Consequently, SC4A-Bu included G1 into its cavity shallowly, affording weaker host–guest interactions than SC4A. The present result agrees well with our previous work that, compared with SC4A, SC4A-Bu shows weaker binding abilities to both the spherical quarterammonium cation (tetramethylammonium) and the spherical neutral molecules (2,3-diazabicyclo[2.2.2]oct-2-ene), originating from the less favourable enthalpy changes (*6*). For SC4A, G1 with two positive charges merits not only the spherical shape complementarity but also the charge complementarity

(*52*), therefore exhibiting the extremely high complexation stability (up to $10^7\,M^{-1}$), governed by both enthalpy and entropy terms. For SC4A-Bu, the spherical shape complementarity disappears but the charge complementarity retains, and then G1 gives merely a medium stability ($10^4\,M^{-1}$), governed by the entropy term. The entropy-driven complexation between SC4A-Bu and G1 indicates that G1 locates at the upper rim, surrounded by sulfonate groups, and the extensive electrostatic-directed desolvation of negatively charged host and positively charged guest acts as the dominant driving force for complexation.

G2, G3 and G4 are all dipyridinium-typed guests. Their aromaticity and planarity decrease in the sequence of G2 > G3 > G4, which fit well with the sequence of the K_S values with SC4A-Bu. This phenomenon indicates that SC4A-Bu is more suitable to encapsulate the planer molecules of large π system with low electron density. For example, G2 shows a host selectivity of 4 (SC4A-Bu/SC4A). Their enthalpy changes are almost the same ($\Delta H^\circ_{SC4A} = -37.6\,kJ\,mol^{-1}$, $\Delta H^\circ_{SC4A\text{-}Bu} = -35.4\,kJ\ mol^{-1}$), but the entropy changes are distinct. SC4A-Bu shows a favourable entropy change, while SC4A shows an unfavourable one ($T\Delta\Delta S^\circ_{SC4A\text{-}Bu-SC4A} = 12.7\,kJ\,mol^{-1}$), resulting from the distinguishable conformation changes of SC4A-Bu and SC4A upon complexation with guest. When binding with G2, the flexible conformation of SC4A was rigidified, and the conformation freedom loss led to an unfavourable entropy change. However, SC4A-Bu has a pre-organised pinched-cone structure, which is suitable for complexation with aromatic planer guests, and therefore the complexation-induced conformation freedom loss would be less than SC4A. The less conformation freedom loss cannot counterbalance the extensive desolvation effect, giving a favourable entropy change.

The complexation of SC4A-Bu with G5 shows the most favourable enthalpy change, possibly because of hydrogen-bonding interactions. When the imidazole ring of G5 was immersed into the calixarene cavity, two N—CH_3 groups are located at the upper rim, surrounded by sulfonate groups. Benefiting from the pinched-cone conformation of SC4A-Bu, two N—CH_3 groups are apt to form multiple non-conventional hydrogen bonds with the sulfonate groups. However, the highly favourable enthalpy term ($-42.2\,kJ\,mol^{-1}$) is offset by the unfavourable entropy term ($-17.3\,kJ\,mol^{-1}$) to much extent, and then SC4A-Bu does not afford such strong binding affinity to G5 as G2–G4. Two factors lead to the considerable entropy loss: comparing with G1–G4, G5 is one positively charged, and the desolvation effect derived from electrostatic interaction of G5 is not as favourable as those of G1–G4; the conformation degree loss upon complexation is large. As a synergistic result of π-stacking, van der Waals, electrostatic as well as hydrogen-bonding interactions, SC4A-Bu and G5 are fixed well to each other, resulting in a pronounced complexation-induced conformation degree loss. G6 is also one positively charged, but possesses one less N—CH_3 group than G5, and therefore G6 offers less opportunity than G5 to form hydrogen bonds with sulfonate groups of SC4A-Bu. The enthalpy change of G6 is obviously less favourable than that of G5 ($\Delta\Delta H^\circ = 10.4\,kJ\,mol^{-1}$). Compensatively, the entropy change of G6 is more favourable than that of G5 ($T\Delta\Delta S^\circ = 13.8\,kJ\,mol^{-1}$). In a previous work (*53*), the formation of a hydrogen bond having an enthalpy change of $-20.9\,kJ\,mol^{-1}$ was found to produce an entropy loss of $-50.22\,kJ\,mol^{-1}$, because hydrogen bond is directional so that the formation of hydrogen bond would make the conformation of the host–guest complex more ordered. So the unfavourable entropy change of G5 with SC4A-Bu would be another assistant evidence for the formation of hydrogen bonds.

At last, we should mention the competitive binding of SC4A or SC4A-Bu with Na^+. As Na^+ present routinely as counterion of the calixarenes in neutral aqueous solution, it is inevitable to consider the complexation of Na^+ with calixarene as a competitive binding scheme (*54*). We measured the K_S value ($275\,M^{-1}$) of SC4A-Bu with Na^+ by performing competitive binding titrations using lucigenin as a competitive dye (Figure S6) (*55*). All these aforementioned ITC experiments were taken at the SC4A-Bu concentration of 0.10 mM. Under such condition, the percentage of free SC4A-Bu was calculated as around 90%, so we ignored the competitive binding with Na^+ when fitting the titration data, although the omnipresent Na^+ would affect the complexation parameters slightly.

Amphiphilic aggregation of SC4A-Bu before and after complexation with G3

SC4A does not show any tendency of self-aggregation in either absence or presence of guests. However, the lower-rim alkyl-modified SC*n*As exhibit an amphiphilic feature. We envisaged that their amphiphilic aggregation behaviour would be affected by the complexation with guests, especially the cation species. As an initial test, we studied the amphiphilic aggregation of SC4A-Bu in the presence of G3. G3 was employed owing to its high complexation stability by SC4A-Bu. It is reported that free SC4A-Bu shows a CAC of 3.18 mM (*28*). Herein, we used Nile red as a fluorescent probe to study the CAC of SC4A-Bu in the presence of G3 (*56*). Taking the 1:1 binding stoichiometry and extremely strong binding affinity into account, the mixing molar ratio between SC4A-Bu and G3 was maintained at 1:1. As shown in Figure 4, upon gradually increasing the concentrations of SC4A-Bu and G3, an inflection point was observed at 0.25 mM. The emission of Nile red enhanced pronouncedly over this concentration, indicating the formation of amphiphilic aggregation with entrapping Nile red into the hydrophobic region. The CAC value of SC4A-Bu upon complexation with G3 decreases

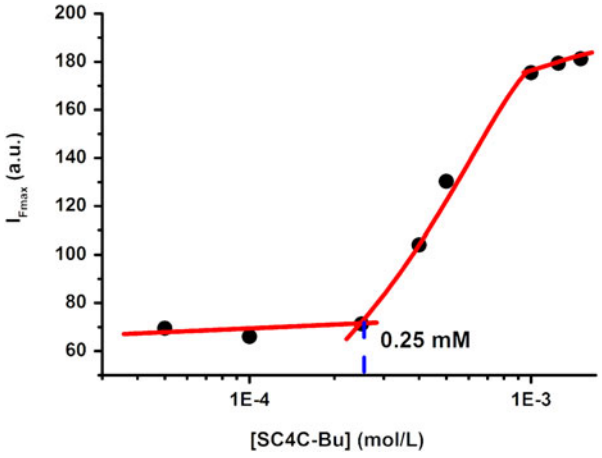

Figure 4. (Colour online) The dependence of fluorescence intensity of Nile red at 650 nm on the SC4A-Bu concentration in the presence of 1 equiv. of G3 (25°C, pH 7.0).

about 12 times, which proves undoubtedly the prediction of guest-regulated amphiphilic aggregation. The systematic investigation on the aggregation of amphiphilic SC*n*As

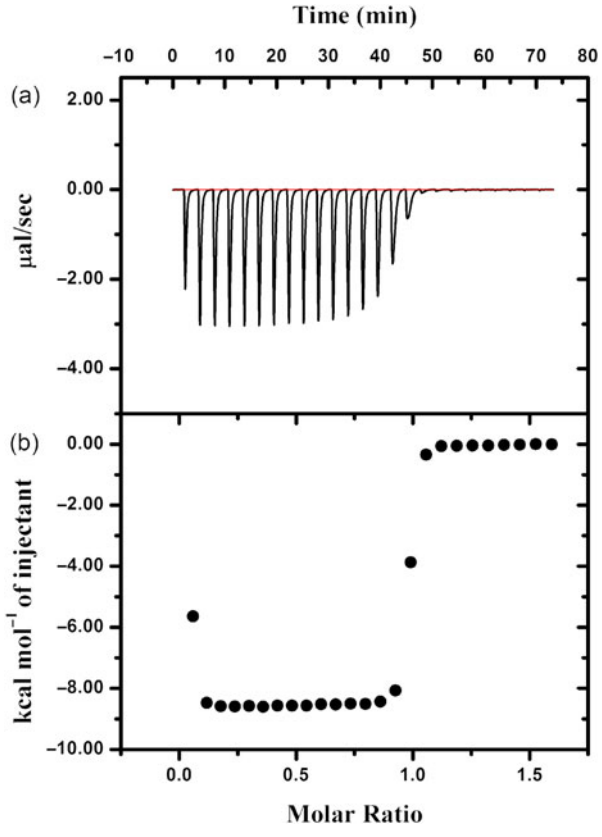

Figure 5. (Colour online) Microcalorimetric titration of SC4A-Bu with G2 at 298.15 K (pH 7.0). (a) Raw data for sequential 25 injections (10 μL per injection) of G2 solution (1.366 mM) injecting into SC4A-Bu solution (0.10 mM). (b) Apparent reaction heat obtained from the integration of calorimetric traces.

derivatives modulated by the complexation of guests is in progress (Figures 5 and 6).

Conclusion

In summary, we investigated the binding ability of an amphiphilic calixarene (SC4A-Bu) with six organic cations (G1–G6) via NMR spectroscopy and ITC. NMR spectra show that lower-rim modification leads to the rigidified pinched-cone conformation adopted by SC4A-Bu and the binding modes of SC4A-Bu and SC4A are similar. However, SC4A-Bu and SC4A show great difference in binding affinities and selectivity. SC4A presents a much stronger binding affinity for G1 than SC4A-Bu with a host selectivity of 688 times, because SC4A-Bu assumes the rigidified pinched-cone conformation and the spherical shape complementarity disappears. The ITC results also show that SC4A-Bu is more suitable to encapsulate the planer molecules of large π system with low electron density, which is mainly driven by the enthalpy term. Furthermore, we studied the amphiphilic aggregation of SC4A-Bu before and after complexation with G3, and found out G3 have an ability to induce the aggregation of SC4A-Bu. The present work would help us design stimuli-responsive amphiphilic assemblies based on calixarenes that modulated by host–guest recognition.

Experimental section

Materials

The host molecules, SC4A (*57*) and SC4A-Bu (*15*), were synthesised and purified according to the respective literature procedures. Six guest molecules, G1 − G6, were synthesised and purified according to the respective literature procedures (*5*, *51*, *58*). Aqueous solutions of pH 7.0 were prepared with distilled, deionised water, adjusted with 1 M NaOH or 1 M HCl. The pH values of solutions were verified with a pH meter calibrated with two standard buffer solutions.

Measurements

NMR spectroscopy

^{1}H NMR spectra were recorded on a Brucker AV400 spectrometer (Bruker Corporation, Germany). Chemical shifts (δ, ppm) in water were externally referenced to 2,2-dimethyl-2-silapentane-5-sulfonate (DSS) in order to avoid any possible interaction with the calixarene hosts as well as with the guests. All the hosts and guests were mixed in the molar ratios of about 1:1, with the guests' concentrations at 2.0 mM. The 2D NMR spectra were recorded on a Varian Mercury VX300 spectrometer (Agilent Technologies Inc., Santa Clara, CA, USA). Samples for 2D NMR were prepared by mixing the guests

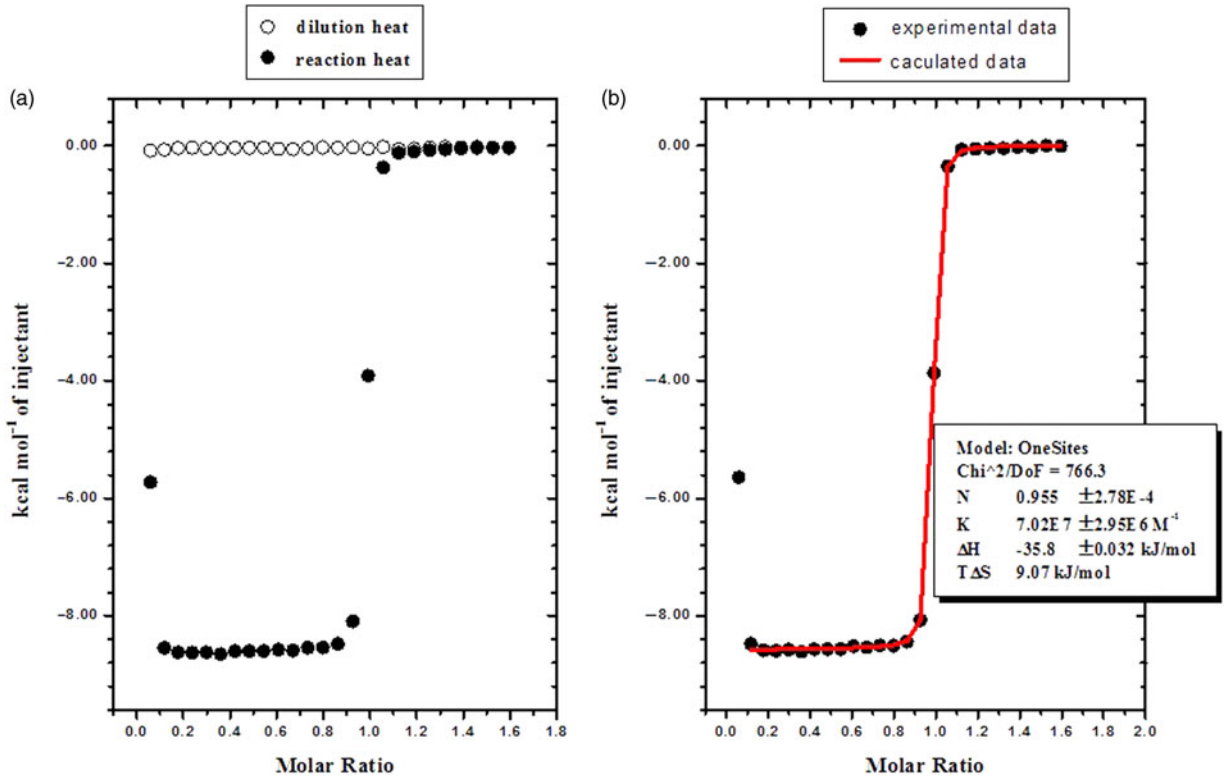

Figure 6. (Colour online) (a) Heat effects of the dilution and of the complexation reaction of G2 with SC4A-Bu at pH 7.0 for each injection during titration microcalorimetric experiment. (b) 'Net' heat effects of complexation of G2 with SC4A-Bu for each injection, obtained by subtracting the dilution heat from the reaction heat, which was fitted by computer simulation using the 'one set of binding sites' model.

and hosts at the molar ratios of 1:1, in which the concentrations of guests/hosts were at 2.0 mM without adding DSS for clarity.

Fluorescence spectroscopy

Steady-state fluorescence spectra were recorded in a conventional quartz cell (light path 10 mm) on a Varian Cary Eclipse spectrometer (Agilent Technologies Inc., Santa Clara, CA, USA) equipped with a Varian Cary single-cell peltier accessory to control temperature. $\lambda_{ex} = 550$ nm; bandwidth (ex), 10 nm; bandwidth (em), 5 nm.

ITC

A thermostated and fully computer-operated isothermal calorimetry instrument, purchased from Microcal Inc., Northampton, MA, was used for all microcalorimetric experiments. All microcalorimetric titrations between hosts and guests were performed in aqueous solution (pH 7.0) at atmospheric pressure and 298.15 K. Each solution was degassed and thermostated by a ThermoVac accessory (Thermo Vac Inc., Dewsbury, West Yorkshire, UK) before the titration experiment. Twenty-five successive injections were made for each titration experiment. A constant volume (10 μL/injection) of guest (or host) solution in a 0.250-mL syringe was injected into the reaction cell (1.4227 mL) charged with host (or guest) solution in the same aqueous solution.

A control experiment was carried out in each run to determine the dilution heat by injecting a guest (or host) aqueous solution into a pure aqueous solution containing no host (or guest) molecules. The dilution heat determined in these control experiments was subtracted from the apparent reaction heat measured in the titration experiments to give the net reaction heat. The net reaction heat in each run was analysed by using the 'one set of binding sites' model (ORIGIN software, Microcal Inc.) to simultaneously compute the binding stoichiometry (N), complex stability constant (K_S), standard molar reaction enthalpy (ΔH°) and standard deviation from the titration curve. Generally, the first point of the titration curve was disregarded, as some liquid mixing near the tip of the injection needle is known to occur at the beginning of each ITC run. Knowledge of the complex stability constant (K_S) and molar reaction enthalpy (ΔH°) enabled the calculation of the standard free energy (ΔG°) and entropy changes (ΔS°) according to

$$\Delta G^\circ = -RT \ln K_S = \Delta H^\circ - T\Delta S^\circ,$$

where R is the gas constant and T is the absolute temperature.

To check the accuracy of the observed thermodynamic parameters, two independent titration experiments were carried out to afford self-consistent thermodynamic parameters, and their average values with associated errors are listed in Table 2.

Funding

This research was financially supported by grants from the National Basic Research Program (also known as the 973 Program) [grant number 2011CB932502] and from the National Natural Science Foundation of China [grant number 91227107], [grant number 21172119], [grant number 21322207].

References

(1) Shinkai, S.; Mori, S.; Tsubaki, T.; Sone, T.; Manabe, O. *Tetrahedron Lett.* **1984**, *25*, 5315–5318.
(2) Guo, D.-S.; Liu, Y. *Acc. Chem. Res.* DOI: 10.1021/ar500009g.
(3) Shinkai, S.; Araki, K.; Matsuda, T.; Nishiyama, N.; Ikeda, H.; Takasu, I.; Iwamoto, M. *J. Am. Chem. Soc.* **1990**, *112*, 9053–9058.
(4) Liu, Y.; Guo, D.-S.; Zhang, H.-Y.; Ma, Y.-H.; Yang, E.-C. *J. Phys. Chem. B* **2006**, *110*, 3428–3434.
(5) Zhao, H.-X.; Guo, D.-S.; Liu, Y. *J. Phys. Chem. B* **2013**, *117*, 1978–1987.
(6) Cui, J.; Uzunova, V.D.; Guo, D.-S.; Wang, K.; Nau, W.M.; Liu, Y. *Eur. J. Org. Chem.* **2010**, 1704–1710.
(7) Paclet, M.H.; Rousseau, C.F.; Yannick, C.; Morel, F.; Coleman, A.W. *J. Inclusion Phenom. Macrocyclic Chem.* **2006**, *55*, 353–358.
(8) Coleman, A.W.; Jebors, S.; Cecillon, S.; Perret, P.; Garin, D.; Marti-Battle, D.; Moulin, M. *New J. Chem.* **2008**, *32*, 780–782.
(9) Perret, F.; Lazar, A.N.; Coleman, A.W. *Chem. Commun.* **2006**, 2425–2438.
(10) Perret, F.; Coleman, A.W. *Chem. Commun.* **2011**, *47*, 7303–7319.
(11) Souchon, V.; Leray, I.; Valeur, B. *Chem. Commun.* **2006**, 4224–4226.
(12) Li, Q.; Guo, D.-S.; Qian, H.; Liu, Y. *Eur J. Org. Chem.* **2012**, 3962–3971.
(13) Atwood, J.L.; Barbour, L.J.; Hardie, M.J.; Raston, C.L. *Coord. Chem. Rev.* **2001**, *222*, 3–32.
(14) Dalgarno, S.J.; Atwood, J.L.; Raston, C.L. *Chem. Commun.* **2006**, 4567–4574.
(15) Shinkai, S.; Mori, S.; Koreishi, H.; Tsubaki, T.; Manabe, O. *J. Am. Chem. Soc.* **1986**, *108*, 2409–2416.
(16) Martin, O.; Yu, L.; Mecozzi, S. *Chem. Commun.* **2005**, 4964–4966.
(17) Bakirci, H.; Koner, A.L.; Dickman, M.H.; Kortz, U.; Nau, W.M. *Angew. Chem. Int. Ed.* **2006**, *45*, 7400–7404.
(18) Hennig, A.; Bakirci, H.; Nau, W.M. *Nat. Methods* **2007**, *4*, 629–632.
(19) Guo, D.-S.; Uzunova, V.; Su, X.; Liu, Y.; Nau, W.M. *Chem. Sci.* **2011**, *2*, 1722–1734.
(20) Ghale, G.; Lanctôt, A.G.; Kreissl, H.T.; Jacob, M.H.; Weingart, H.; Winterhalter, M.; Nau, W.M. *Angew. Chem. Int. Ed.* **2014**, *53*, 2762–2765.
(21) Guo, D.-S.; Yang, J.; Liu, Y. *Chem. Eur. J.* **2013**, *19*, 8755–8759.
(22) Koh, K.N.; Araki, K.; Ikeda, A.; Otsuka, H.; Shinkai, S. *J. Am. Chem. Soc.* **1996**, *118*, 755–758.
(23) Arena, G.; Casnati, A.; Contino, A.; Magrì, F.; Sansone, A.; Sciotto, D.; Ungaro, R. *Org. Biomol. Chem.* **2006**, *4*, 243–249.
(24) Helttunena, K.; Shahgaldian, P.; New *J. Chem.* **2010**, *34*, 2704–2714.
(25) Liang, Q.; Guan, B.; Jiang, M. *Prog. Chem.* **2010**, *22*, 388–399.
(26) Qin, Z.; Guo, D.-S.; Gao, X.-N.; Liu, Y. *Soft Matter* **2014**, *10*, 2253–2263.
(27) Basilio, N.; Francisco, V.; García-Río, L. *Int. J. Mol. Sci.* **2013**, *14*, 3140–3157.
(28) Basilio, N.; García-Río, L. *ChemPhysChem.* **2012**, *13*, 2368–2376.
(29) Kellermann, M.; Bauer, W.; Hirsch, A.; Schade, B.; Ludwig, K.; Bottcher, C. *Angew. Chem. Int. Ed.* **2004**, *43*, 2959–2962.
(30) Basilio, N.; García-Río, L.; Martín-Pastor, M. *J. Phys. Chem. B* **2010**, *114*, 4816–4820.
(31) Zadmard, R.; Schrader, T. *J. Am. Chem. Soc.* **2005**, *127*, 904–915.
(32) Wang, Y.-X.; Guo, D.-S.; Cao, Y.; Liu, Y. *RSC Adv.* **2013**, *3*, 8058–8063.
(33) Houmadi, S.; Coquière, D.; Legrand, L.; Fauré, M.C.; Goldmann, M.; Reinaud, O.; Rémita, S. *Langmuir* **2007**, *23*, 4849–4855.
(34) Guo, D.-S.; Wang, K.; Wang, Y.-X.; Liu, Y. *J. Am. Chem. Soc.* **2012**, *134*, 10244–10250.
(35) Guo, D.-S.; Jiang, B.-P.; Wang, X.; Liu, Y. *Org. Biomol. Chem.* **2012**, *10*, 720–723.
(36) Wang, K.; Guo, D.-S.; Wang, X.; Liu, Y. *ACS Nano* **2011**, *5*, 2880–2894.
(37) Wang, K.; Guo, D.-S.; Liu, Y. *Chem. Eur. J.* **2010**, *16*, 8006–8011.
(38) Jiang, B.-P.; Guo, D.-S.; Liu, Y.-C.; Wang, K.-P.; Liu, Y. *ACS Nano* **2014**, *8*, 1609–1618.
(39) Wang, K.; Guo, D.-S.; Zhao, M.-Y.; Liu, Y. *Chem. Eur. J.* **2013** DOI: 10.1002/chem.201303963.
(40) Li, Z.-Q.; Hu, C.-X.; Cheng, Y.-Q.; Xu, H.; Cao, X.-L.; Song, X.-W.; Zhang, H.-Y.; Liu, Y.; Chem *J. Chin. Univ.* **2013**, *34*, 91–95.
(41) Consoli, G.M.L.; Cunsolo, F.; Geraci, C.; Mecca, T.; Neri, P. *Tetrahedron Lett.* **2003**, *44*, 7467–7470.
(42) Consoli, G.M.L.; Cunsolo, F.; Geraci, C.; Sgarlata, V. *Org. Lett.* **2004**, *6*, 4163–4166.
(43) Lee, M.; Lee, S.-J.; Jiang, L.-H. *J. Am. Chem. Soc.* **2004**, *126*, 12724–12725.
(44) Schuehle, D.T.; Schatz, J.; Laurent, S.; Vander Elst, L.; Mueller, R.; Stuart, M.C.A.; Peters, J.A. *Chem. Eur. J.* **2009**, *15*, 3290–3296.
(45) DaSilva, E.; Coleman, A.W. *Tetrahedron* **2003**, *59*, 7357–7364.
(46) Arena, G.; Casnati, A.; Mirone, L.; Sciotto, D.; Ungaro, R. *Tetrahedron Lett.* **1997**, *38*, 1999–2002.
(47) Sansone, F.; Barboso, S.; Casoati, A.; Sciotto, D.; Ungaro, R. *Tetrahedron Lett.* **1999**, *40*, 4741–4744.
(48) Kalchenko, O.I.; DaSilva, E.; Coleman, A.W. *J. Inclusion Phenom. Macrocyclic Chem.* **2002**, *43*, 305–310.
(49) Koblenz, T.S.; Dekker, H.; de Koster, C.; Leeuwen, P.; Reek, J. *Chem. Commun.* **2006**, 1700–1702.
(50) Arena, G.; Casnati, A.; Contino, A.; Lombardo, G.G.; Sciotto, D.; Ungaro, R. *Chem. Eur. J.* **1999**, *5*, 738–744.

(51) Wang, K.; Guo, D.-S.; Zhang, H.-Q.; Li, D.; Zheng, X.-L.; Liu, Y. *J. Med. Chem.* **2009**, *52*, 6402–6412.
(52) Bakirci, H.; Korner, A.L.; Nau, W.M. *J. Org. Chem.* **2005**, *70*, 9960–9966.
(53) Gilli, P.; Ferretti, V.; Gilli, G. *J. Phys. Chem.* **1994**, *98*, 1515–1518.
(54) Francisco, V.; Piñeiro, A.; Nau, W.M.; García-Río, L. *Chem. Eur. J.* **2013**, *19*, 17809–17820.
(55) Bakirci, H.; Koner, A.L.; Nau, W.M. *Chem. Commun.* **2005**, 5411–5413.
(56) Coutinho, P.; Castanheira, E.; Rei, M.; Oliveira, M. *J. Phys. Chem. B* **2002**, *106*, 12841–12846.
(57) Arena, G.; Contino, A.; Lombardo, G.G.; Sciotto, D. *Thermochim. Acta* **1995**, *264*, 1–11.
(58) Xiao, Y.; Chu, L.; Sanakis, Y.; Liu, P. *J. Am. Chem. Soc.* **2009**, *131*, 9931–9933.